Hindawi
Advances in Materials Science and Engineering
Volume 2017, Article ID 1691465, 13 pages
https://doi.org/10.1155/2017/1691465

Research Article

Statistical Model for the Mechanical Properties of Al-Cu-Mg-Ag Alloys at High Temperatures

A. M. Al-Obaisi,[1,2] E. A. El-Danaf,[1] A. E. Ragab,[3] M. S. Soliman,[1] and A. N. Alhazaa[4,5]

[1] *Mechanical Engineering Department, College of Engineering, King Saud University, P.O. Box 800, Riyadh 11421, Saudi Arabia*
[2] *Mechanical Engineering Department, King Abdulaziz University, Jeddah, Saudi Arabia*
[3] *Industrial Engineering Department, College of Engineering, King Saud University, P.O. Box 800, Riyadh 11421, Saudi Arabia*
[4] *Physics & Astronomy Department, Faculty of Science, King Saud University, P.O. Box 2455, Riyadh 11451, Saudi Arabia*
[5] *King Abdullah Institute for Nanotechnology (KAIN), King Saud University, Riyadh, Saudi Arabia*

Correspondence should be addressed to E. A. El-Danaf; edanaf@ksu.edu.sa

Received 2 March 2017; Revised 15 May 2017; Accepted 1 June 2017; Published 9 July 2017

Academic Editor: Markus Bambach

Aluminum alloys for high-temperature applications have been the focus of many investigations lately. The main concern in such alloys is to maintain mechanical properties during operation at high temperatures. Grain coarsening and instability of precipitates could be the main reasons behind mechanical strength deterioration in these applications. Therefore, Al-Cu-Mg-Ag alloys were proposed for such conditions due to the high stability of Ω precipitates. Four different compositions of Al-Cu-Mg-Ag alloys, designed based on half-factorial design, were cast, homogenized, hot-rolled, and isothermally aged for different durations. The four alloys were tensile-tested at room temperature as well as at 190 and 250°C at a constant initial strain rate of 0.001 s^{-1}, in two aging conditions, namely, underaged and peak-aged. The alloys demonstrated good mechanical properties at both aging times. However, underaged conditions displayed better thermal stability. Statistical models, based on fractional factorial design of experiments, were constructed to relate the experiments output (yield strength and ultimate tensile strength) with the studied process parameters, namely, tensile testing temperature, aging time, and copper, magnesium, and silver contents. It was shown that the copper content had a great effect on mechanical properties. Also, more than 80% of the variation of the high-temperature data was explained through the generated statistical models.

1. Introduction

For decades, the market of lightweight materials has been growing and enlarging year by year, due to the increasing demand for energy saving. Aluminum alloys are still one of the main lightweight materials under investigation. Development and design of high strength aluminum alloys to operate at elevated temperatures is getting great attention. Applications for high-temperature aluminum alloys include supersonic aviation and automotive components. However, stability of precipitates at high temperature is still a major concern. Strength at elevated temperature starts to deteriorate after a specific time because of precipitates coarsening. Thus, the objective of many researches, recently, is to develop and design new aluminum alloys with precipitates that are stable at high temperatures. The use of Al-Cu-Mg-Ag aluminum alloys (AA2139 and AA2519) has increased substantially in aircraft and military applications due to their low density, exceptional toughness, and moderately high-temperature stability [1–3].

The Concorde was the most famous supersonic civil aircraft. It was adopted by French and British Airways. The Concorde alloy was 2618A (Al-2.2%Cu-1.5%Mg-1%Fe-1%Ni-0.2%Si). The precipitates of 2618A are stable at elevated temperature and this is the reason behind choosing this alloy; even so, the mechanical properties are not in the same level when compared with conventional aerospace aluminum alloys like 2024-T6 and 7075-T6 [4]. The temperature on the skin of the airplane body is about 127°C, due to air friction at a speed of Mach 2.05 [5]. Despite its speed, the Concorde failed economically, because it can only carry up to 100 passengers and was not able to fly for a long distance.

Therefore, Al-Cu-Mg-Ag system was proposed to replace 2618A and other conventional aerospace aluminum alloys, 2024-T6 and 7075-T6, in view of the fact that these new alloys give high thermal stability and good mechanical properties [5, 6]. Many recent publications [1, 7, 8] have focused on investigating the evolution of microstructure and mechanical properties in these alloys.

A superior combination of high thermal stability and good mechanical properties comes from special precipitates called Ω [5]. Bakavos et al. [9] used transmission electron microscopy (TEM) to explore the habit planes of Ω precipitates. It was found that the habit planes of Ω with the matrix are $\{111\}_\alpha$. Regarding the morphology of Ω precipitates, Lumley and Polmear [10] stated that Ω has an orthorhombic plate-like shape. For the composition of Ω phase, researchers are still uncertain about it. Lumley and Polmear [10] mentioned that the composition of Ω was close to that of Al_2Cu with Mg and Ag detected at α/Ω interfaces. Gable et al. [11] studied the stability of Ω phase at different aging temperatures of 200 and 250°C. It was shown that the density of Ω phase plates decreases intensely if the alloy is aged at a temperature at 250°C or higher for 30 minutes or longer. Also, Gable et al. [11] showed that the thickness of Ω phase increases significantly if the alloy is aged at 250°C. Xiao et al. [12] confirmed this observation where the Ω phases are thermally stable at temperatures below 200°C.

Bakavos et al. [9] investigated the precipitates of two alloys of Al-Cu-Mg with and without silver (Ag) addition. It was stated that the Ω phase was observed in both alloys. However, Ω phases in Al-Cu-Mg-Ag were finer compared with Al-Cu-Mg free of Ag. Gable et al. [11] showed that the content of Ω phase is related to the content of Mg. Ω phase works with the other well-known precipitates θ' and S to enhance the mechanical properties significantly. The habit planes of θ' phases are $\{001\}_\alpha$ and have a composition of Al_2Cu and tetragonal plate-like shape [9, 13]. For S phases, the habit planes are $\{001\}_\alpha$ and have a composition of Al_2CuMg and a cubic shape [10]. The dominant phases in the Al-Cu-Mg-Ag system which has a great effect on enhancing the mechanical properties are Ω and then θ'. S has minor significance [10]. It has been shown [14] that the precipitation sequence is as follows:

$$\text{GP zones} \longrightarrow \theta'' \longrightarrow \theta' + \Omega \longrightarrow \theta' + S' \longrightarrow S + \theta. \quad (1)$$

Song et al. [15] studied the mechanical properties of three alloys, A2618 (Al-2.2%Cu-1.5%Mg-1%Fe-1%Ni-0.2%Si), Al-8Cu-0.5Mg free of Ag, and Al-8Cu-0.5Mg-0.6Ag, at a wide range of temperatures from 20 to 300°C. It was shown that the alloy with the addition of low content of Ag has better mechanical properties at low and high temperatures compared with other alloys. Xia et al. [16] investigated the effect of heat exposure on the mechanical properties of the aged alloy (Al-4.72Cu-0.45Mg-0.54Ag-0.17Zr). The aging process was conducted at a temperature of 165°C for 2 h (underaged condition). The heat exposure was implemented at 200°C for different times of exposure starting from zero to 100 h. It was shown that there was an initial increase in strength with increasing duration of heat exposure, whereas after 10 h the strength started to decrease. The ultimate tensile stress (UTS) after 100 h of exposure was about 400 MPa, whereas it was 430 MPa before exposure [16].

Liu et al. [17] studied the creep behavior of Al-5.33Cu-0.79Mg-0.48Ag-0.30Mn-0.14Zr. The study on the three alloys was conducted at a temperature of 150°C as well as at stress of 150 to 300 MPa for underaged conditions. It was shown that the steady creep rates were 0.12, 0.06, 0.03, and 0.01% per hour at 150, 200, 250, and 300 MPa, respectively [17]. Lumley et al. [18] explored the creep behavior of two alloys, that is, traditional aviation aluminum alloy (Al 2024) and experimental alloy with composition of Al-5.6Cu-0.45Mg-0.45Ag-0.3Mn-0.18Zr for two different aging conditions of underaged and fully hardened (T6) conditions. The creep test parameters were temperature of 300°C and stress of 150 MPa. It was obvious that the underaged condition gave a lower creep rate for both alloys. Al 2024 displayed secondary creep after 200 h and 400 h for T6 and underaged conditions, respectively, while the experimental alloy with low content of Ag did not show a secondary creep behavior for both aging conditions. Based on this result, Lumley and Polmear [10] investigated the creep behavior of underaged conditions for the previous experimental alloy that contained a low amount of Ag extensively at different creep circumstances. The creep test condition was a temperature of 130°C and stress of 200 MPa for 20000 h. It was represented that the creep rate percentage was about 0.4 and there was no secondary creep observed along the duration of the test [10].

Al-Obaisi et al. [19] studied the aging characteristic of eight different compositions of Al-Cu-Mg-Ag based on full-factorial design at three different aging temperatures of 160, 190, and 220°C for a wide range of aging durations. Statistical modeling was constructed between hardness values and process inputs comprising aging temperatures and times, as well as weight percentages of alloying elements through Minitab software. It was presented that changing of weight percentages of alloying elements changed the hardness values significantly. Also, it was deduced that aging at 190°C gave good hardness values with reasonable aging duration that could be appealing to industry needs [19]. This temperature was used as an aging temperature for the current study.

Most researchers focused on studying the mechanical properties of a single composition of Al-Cu-Mg-Ag and mostly at one aging condition. A complete study of mechanical properties at high temperatures for different aging conditions and different compositions of Al-Cu-Mg-Ag is still required. This is the stimulation for the current work. Based on the fractional factorial design of the experiment, four alloys were prepared. They were tensile-tested at room temperature, 190°C, and 250°C and at two different aging conditions (underaged and peak-aged). Thus, the mechanical properties of the four alloys were related to the process parameters (tensile testing temperature, aging time, and alloying elements percentage) through statistical modeling.

Table 1: Chemical compositions of the used alloys.

Alloy number	wt.% Cu	wt.% Mg	wt.% Ag	wt.% Al
1	5.0 (+)	0.5 (−)	0.3 (−)	Balance
2	3.0 (−)	1.0 (+)	0.3 (−)	Balance
3	3.0 (−)	0.5 (−)	0.6 (+)	Balance
4	5.0 (+)	1.0 (+)	0.6 (+)	Balance

Table 2: Chemical analysis of the investigated alloys (wt.%)*.

Alloy number	Cu	Mg	Ag	Al	Cu/Mg ratio
1	5.29	0.46	0.30	Balance	11.5
2	3.24	0.95	0.31	Balance	3.4
3	3.15	0.47	0.62	Balance	6.8
4	5.11	0.96	0.61	Balance	5.32

*The rest of the alloying elements had the percentages Si ≤ 0.05, Fe ≤ 0.2, Ni ≤ 0.03, Cr ≤ 0.056, Zn ≤ 0.031, Ti ≤ 0.016, and Mn ≤ 0.006.

Table 3: Aging time for each aging condition.

Alloy number	Underaged		Peak-aged	
	Aging time	Hardness (HV)	Aging time	Hardness (HV)
1	30 min	124	2 h	167
2	30 min	103	2 h	132
3	30 min	97	8 h	127
4	10 min	165	1 h	172

2. Methodology

2.1. Materials Preparation. Three alloying elements, namely, Cu, Mg, and Ag, were added to Al, with two levels for each, (−) and (+), based on fractional factorial design. Since it is a fractional factorial design, four alloys with compositions presented in Table 1 were cast in a steel mold. If a full factorial was employed, eight alloys would have been required [19]. The dimensions of the cast ingots were 100 × 40 × 15 mm. The homogenizing process was conducted at 540°C for 24 h. The four alloys were elementally analyzed through arc and spark excitation and the chemical analysis is displayed in Table 2. Then, the four alloys were hot-rolled at 450°C. During the rolling process, 80% of the total thickness was reduced.

Tensile samples were wire-cut from the rolled alloys such that the tensile axis was parallel to the rolling direction. The tensile samples had a gage length of 10 mm and a cross-sectional area of 4 × 1.5 mm^2. Solution treatment was carried out at a temperature of 540°C for Alloys 1 and 4 that have a higher content of Cu (5 wt.%) and at 500°C for Alloys 2 and 3 that have a low content of Cu (3 wt.%) to make sure that all four alloys were taken to a single phase region. Then, the four alloys were water-quenched. The aging process was implemented in a salt bath constituted of 50% potassium nitrate (KNO_3) and sodium nitrite ($NaNO_2$) at a temperature of 190°C with different aging times, and then the samples were water-quenched. The corresponding hardness values and aging times are displayed in Table 3. Tensile testing was performed for each sample at room temperature, 190°C, and 250°C for each aging condition. The tensile test was carried out on an Instron machine model 3388 equipped with a data monitoring system. The testing temperature is controlled to be within ±2°C. The tensile data is processed using an Excel sheet and corrected for machine compliance.

The microstructure study was performed using SEM model JEOL 6610 LV and TEM JEOL model JEM-2100F-HR, operated at 200 kV. Thin foil, ~300 nm thickness, for TEM investigation was prepared using focused ion beam system (JEOL JEM9320 FIB).

2.2. Design of Experiments (DOE). Fractional factorial is a well-known technique to be used in material and manufacturing experimentation. Several researchers made use of the technique in the process of investigating the significant factors in experiments [20–22]. A fractional factorial design reduces significantly the number of runs required, particularly in screening experiments where many factors are studied in order to decide the relative importance amongst them. The price of this reduction in the number of runs is the sacrifice of some higher order interactions.

In this research, a 2^{k-1} fractional factorial design was used with five factors, two levels each. The number of runs needed is 16 runs compared to 32 runs in a full-factorial (2^k) design. The factors and levels evaluated in the research are listed in Table 4. Four numerical factors are used, namely, testing temperature and Cu, Mg, and Ag wt.%. The fifth factor (aging time) was treated as a categorical parameter rather than numerical since the aging time for each alloy was different. Its levels are given as U (−1) and P (+1). It is worth noting that the model was built to study, solely, the high-temperature mechanical properties.

Table 4: Factors and their levels in the experiment fractional factorial design for the high-temperature study.

Factors	Index	Levels	
		Low (−1)	High (+1)
Aging time	*A*	Underaged (U)	Peak-aged (P)
Testing temperature (°C)	*B*	190	250
Cu (wt.%)	*C*	3.0	5.0
Mg (wt.%)	*D*	0.5	1.0
Ag (wt.%)	*E*	0.3	0.6

Table 5: Mechanical properties at room and high temperatures for each aging condition of all four alloys.

Alloy number	Testing temp. (°C)	Yield strength (MPa)		Ultimate tensile strength (UTS) (MPa)	
		Underaged	Peak-aged	Underaged	Peak-aged
1	20°C	305	420	412	480
	190°C	315	350	354	372
	250°C	250	247	260	247
2	20°C	260	275	366	385
	190°C	250	210	310	237
	250°C	200	190	214	195
3	20°C	265	310	352	359
	190°C	190	250	220	271
	250°C	190	185	201	195
4	20°C	300	400	405	447
	190°C	295	320	320	341
	250°C	200	210	220	245

3. Results and Discussion

3.1. Mechanical Properties. Figures 1(a)–1(c) represent examples of the engineering stress-strain curves for Alloy 4 tested at room temperature (a), 190°C (b), and 250°C (c), respectively, for the underaged and peak-aged conditions at 190°C.

Table 5 summarizes the yield strength (YS) and ultimate tensile strength (UTS) values for each aging condition of all four alloys at room and high temperatures. As expected, the stress values decrease with temperature. For ultimate tensile strength (UTS) values, Alloy 1 gave the highest values for both underaged and peak-aged conditions. However, Alloy 3 gave the lowest values. The difference between Alloy 1 and Alloy 3 was around 120 MPa at room temperature and about 50 MPa at high temperature for peak-aged conditions, while for underaged conditions the difference was about 60 MPa at both room and high temperatures. For yield strength (YS) values, Alloy 1 gave the highest values while Alloy 2 gave the lowest values at room temperature, but Alloy 3 exhibited the lowest values at high temperature. The difference between Alloy 1 and Alloy 2 was around 145 and 45 MPa at room temperature for peak-aged and underaged conditions, respectively. For high temperature, the difference between Alloys 1 and 3 was about 60 MPa for both aging conditions. Mostly, the stress values of peak-aged conditions were higher than of underaged conditions except at a temperature of 250°C at which underaged conditions were higher, while in Alloy 2 the underaged condition is more superior compared to the peak-aged condition at both 190 and 250°C. In Alloy 4, stress values of the peak-aged condition were higher than of the underaged condition at all testing temperatures.

Figures 2–5 show the sensitivity of mechanical properties (UTS and YS) with temperatures of both underaged and peak-aged conditions of all four alloys. The data was linearly fitted and the negative slope was taken as an indicator of the thermal stability, in a sense that smaller negative slope can be interpreted as higher thermal stability. The negative slopes of yield strength for underaged conditions were between −0.17 and −0.37. Alloys 3 and 4 had the highest negative slopes, while Alloys 1 and 2 had the lowest negative slopes. However, the negative slopes of ultimate tensile strength (UTS) for underaged conditions were between −0.59 and −0.74. Alloys 3 and 4 had the highest negative slopes, while Alloys 1 and 2 had the lowest negative slopes.

The sensitivity of mechanical properties with temperatures of the peak-aged condition for all four alloys is as follows. For yield strength, the negative slopes were between −0.37 and −0.75. Alloys 1 and 4 had the highest negative slopes, while Alloys 2 and 3 had the lowest negative slopes. However, the negative slopes of ultimate tensile strength (UTS) were between −0.67 and −0.93. Alloys 1, 2, and 4 had higher negative slopes, while Alloy 3 had a lower negative slope. It is obvious that the sensitivity of peak-aged conditions is larger than of the underaged condition, which indicates that

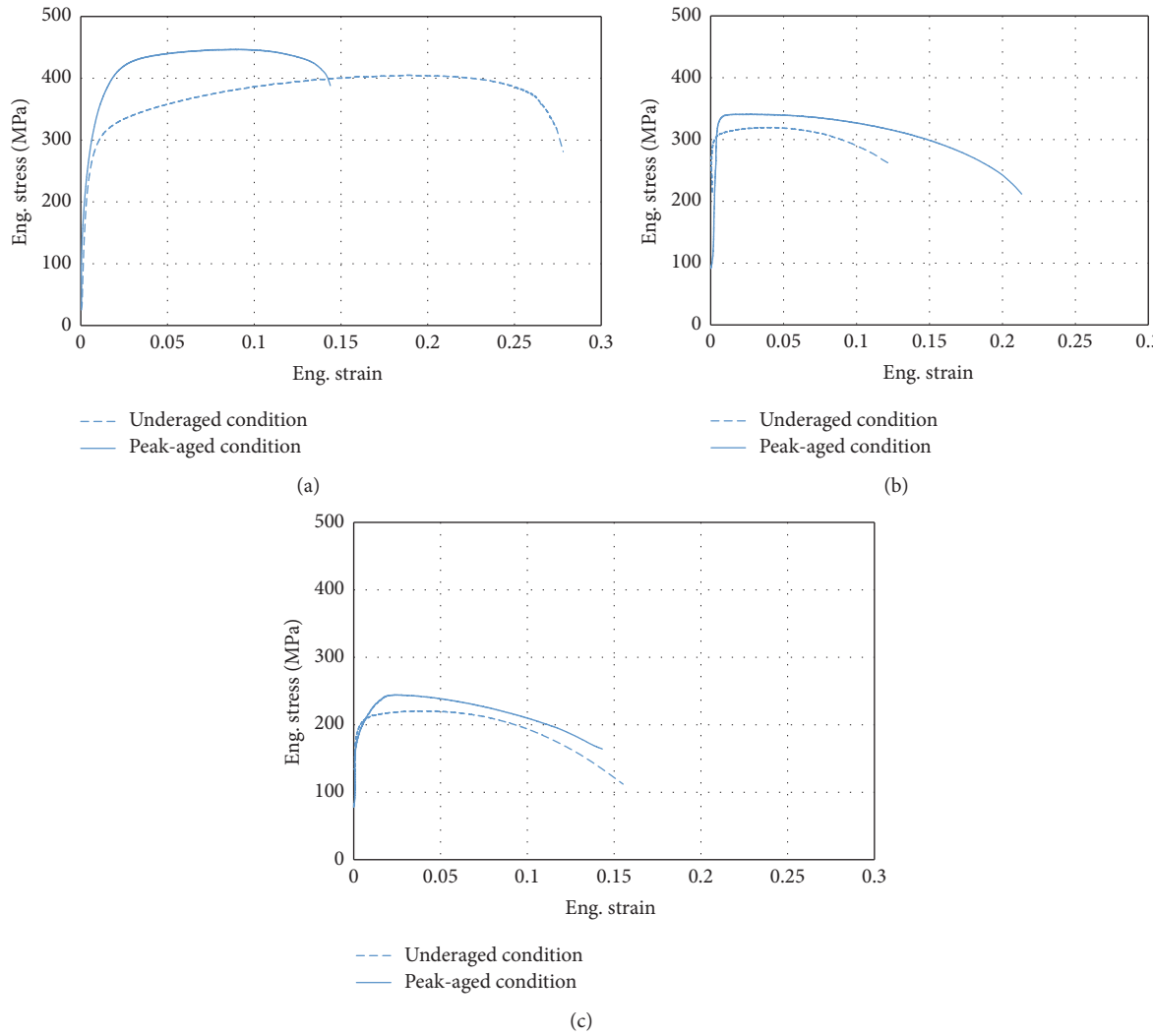

Figure 1: (a) Eng. stress-strain curves of Alloy 4 tested at room temperature for both aging conditions. (b) Eng. stress-strain curves of Alloy 4 tested at 190°C for both aging conditions. (c) Eng. stress-strain curves of Alloy 4 tested at 250°C for both aging conditions.

the underaged condition exhibits higher thermal stability. These observations are consistent with the results of Bai et al. [13].

It would be beneficial to estimate the behavior of the Al-Cu-Mg-Ag system by comparing it with the Concorde alloy (A2618). The following data is extracted from [10]. It was shown that the yield strength values at 20, 150, 200, and 250°C were 372, 303, 179, and 62 MPa, respectively. For ultimate tensile strength, the values were 441, 345, 221, and 90 MPa. The negative slope of the relation between yield strength and temperatures is −1.3, while for ultimate tensile strength it is −1.46. Therefore, Alloys 1 and 4 of peak-aged conditions, from the current study, gave better mechanical properties and lower sensitivity to temperatures. Also, it will be of interest to compare the present results with the behavior of Al 7075, which is one of the high strength aerospace aluminum alloys, at high temperatures. Polmear and Couper [23] showed that the yield strength of this alloy at room temperature is about 500 MPa, while at 190 and 250°C the yield strength is 200 and 50 MPa, respectively. Thus, the performance of this alloy is catastrophic at high temperatures.

The superior thermal stability for some of the current alloys is attributed to a special new phase named Ω that forms as thin platelet precipitates on $\{111\}_\alpha$ planes (α is an Al-based solid solution) and has either a hexagonal or an orthorhombic shape [24–26]. Since $\{111\}_\alpha$ are slip planes in α Al-based solid solution alloys, precipitation of Ω in these alloys tends to improve resistance to dislocation slip and improve mechanical properties [27].

3.2. Microstructure. A TEM study was conducted on Alloy 4 in the peak-aged condition as presented in Figure 6. Figure 6(a) represents a STEM dark field image of the alloy which shows the precipitated phases in bright color exhibiting different morphologies (rod and spherical shaped). The size of the precipitates ranged from 200 to 300 nm. Figure 6(b) presents an EDS spectrum taken at one of these particles, showing the elemental composition in wt.% to be Al 94.2, Cu

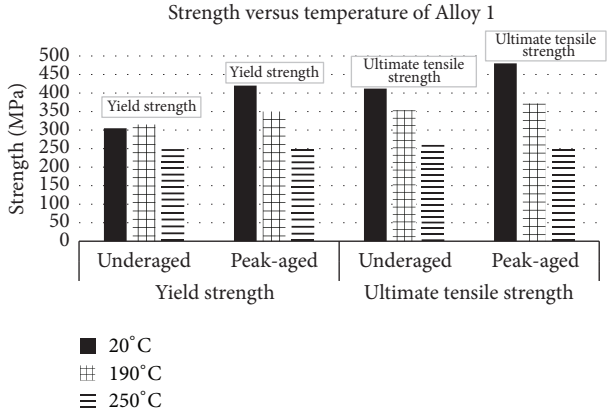

Figure 2: Yield strength (YS) and ultimate tensile strength (UTS) at various temperatures for both aging conditions of Alloy 1.

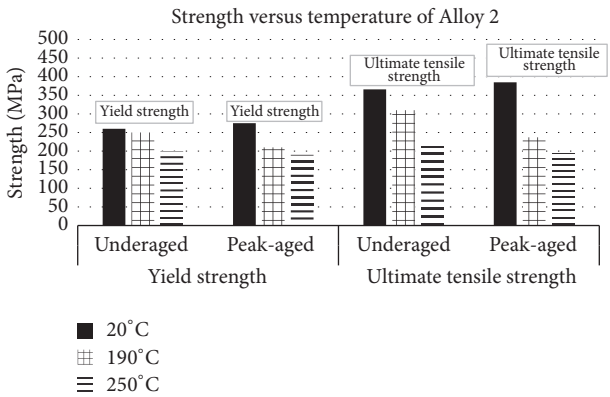

Figure 3: Yield strength (YS) and ultimate tensile strength (UTS) at various temperatures for both aging conditions of Alloy 2.

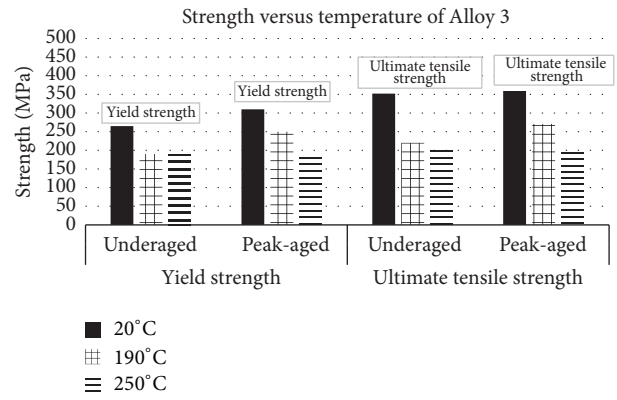

Figure 4: Yield strength (YS) and ultimate tensile strength (UTS) versus temperature for both aging conditions of Alloy 3.

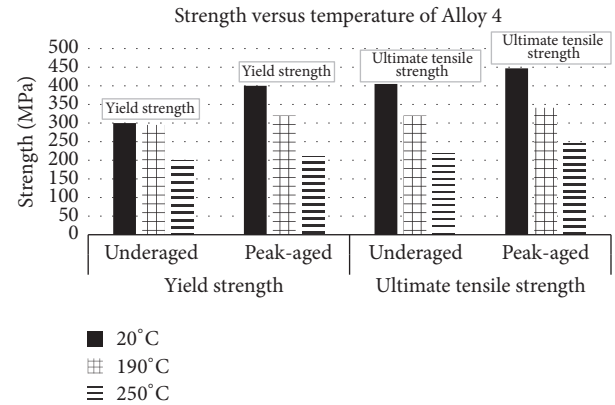

Figure 5: Yield strength (YS) and ultimate tensile strength (UTS) versus temperature for both aging conditions of Alloy 4.

4.3, and Ag 1.5 wt.%. The amount of Mg was not detectable as it could be traces. This particle could be an Ω phase, according to the definition previously mentioned.

A detailed fractography investigation was carried out for Alloy 2, since its mechanical properties were more thermally stable for the two aging conditions. Figure 7 shows SEM images of the fractured surfaces of Alloy 2 tested at room temperature, 190°C, and 250°C, respectively, for different aging conditions. The images of the underaged conditions for all testing temperatures show that the dominant fracture mode is transgranular fracture regarding the observed dimples along the fracture surfaces. These dimples become shallow at higher testing temperatures. For peak-aged conditions, the fractured surfaces show a combined fracture mode including transgranular and intergranular fracture modes. This observation is consistent with the deduction that the underaged conditions are more thermally stable compared with peak-aged conditions. Some of the particles distributed on the fractured surfaces were chemically analyzed through energy dispersion spectroscopy (EDS) technique. Figure 8 shows the EDS spectrum of one of the particles distributed on the fractured surface of Alloy 2 tested at room temperature for the peak-aged condition. The particle size is about 1 μm. The EDS spectrum displays clustering of Cu and Al atoms and to a much lesser extent the Mg and Ag atoms which could imply a coarsened phase of Ω precipitates. Figure 9 presents the EDS spectrum of one of the particles distributed on the fractured surface of Alloy 2 tested at 250°C for the peak-aged condition. The particle size is about 1 μm. The EDS spectrum exhibits clustering of Cu, Mg, and Al atoms which suggests a coarsened phase of *S* precipitates.

3.3. Statistical Analysis. To prepare the fractional factorial design matrix, a full-factorial design was built for the basic factors (*A*, *B*, *C*, and *D*) and a generator ($E = CD$) was used to define the levels of the remaining factor (E) in the matrix. Generators are, mainly, interactions of the basic factors that determine how a subset of experiments is selected from full set runs. The alias structure, given in Table 6, illustrates the confounding between factors and interactions due to the reduction in total runs in a fractional factorial design.

The set of experiments with measured responses is illustrated in Table 7. Responses yield strength and ultimate tensile strength are indexed as *Y* and *U*, respectively. Since the design did not include replicates, the third-, fourth-, and fifth-level interactions were removed to free some

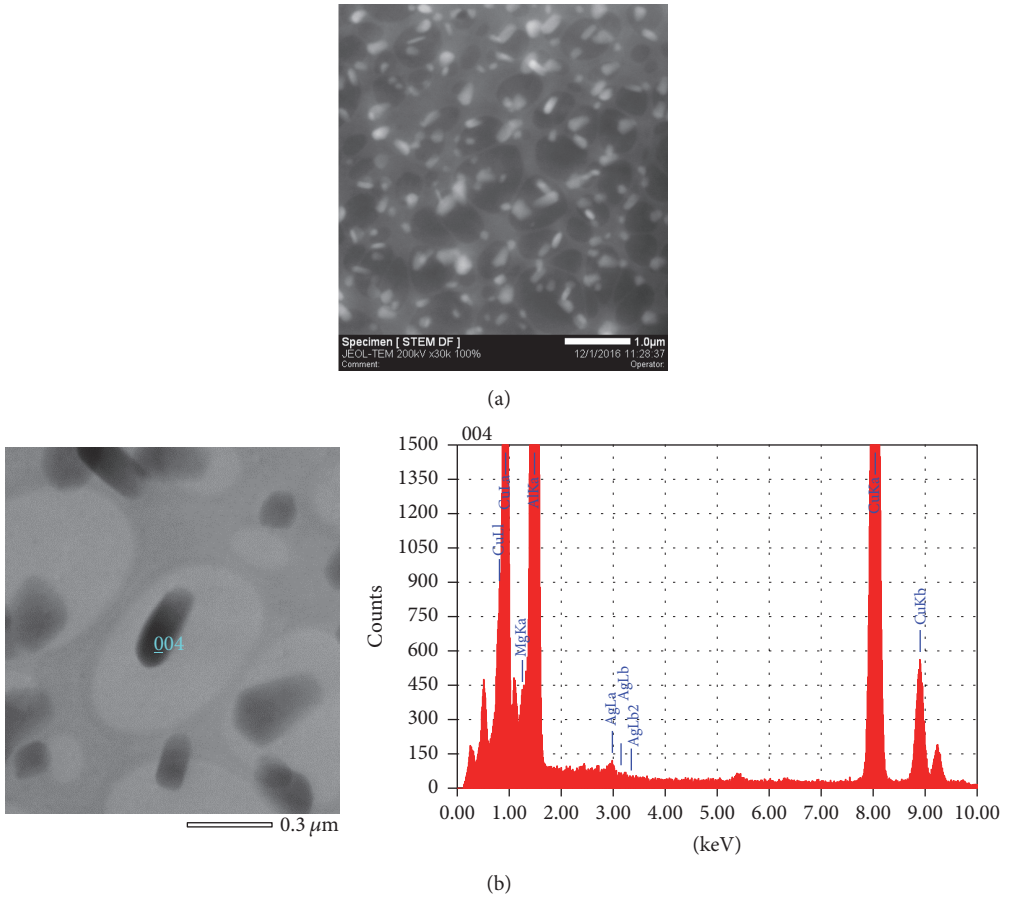

Figure 6: (a) STEM dark field image for Alloy 4 in the peak-aged condition. (b) EDS spectrum for the elemental composition of one selected precipitate.

Table 6: Alias structure for the high-temperature study.

Contrast	Estimates
1	$A + ACDE$
2	$B + BCDE$
3	$C + DE$
4	$D + CE$
5	$E + CD$
6	AB
7	$AC + ADE$
8	$AD + ACE$
9	$AE + ACD$
10	$BC + BDE$
11	$BD + BCE$
12	$BE + BCD$
13	$ABC + ABDE$
14	$ABD + ABCE$
15	$ABE + ABCD$

degrees of freedom for error estimation in order to test the significance of the effects of more important factors and second-order interactions. Analysis of variance was used to estimate the significance of each factor and interaction. Regression analysis was conducted to correlate each response to its significant parameters.

Analysis of variance (ANOVA) was used to decide which model terms (representing the studied process parameters and their interactions) affect significantly the experimental outputs. In ANOVA, the role of each term in the variability of experimental outputs is calculated as its adjusted sum of squares (Adj. SS). The value of Adj. SS of each term with respect to the total Adj. SS represents the contribution of this term to the total variability. Adj. MS for each term represents an estimate of population variance and is calculated by dividing its Adj. SS by its degrees of freedom. The F-value is then calculated for each term by dividing its Adj. MS by the error Adj. MS. A higher F-value indicates that the data contradicts more the test null hypothesis (which assumes nonsignificance of the considered term.) Another item to be calculated is the P value. A lower P value corresponds to a higher F-value. P value less than the test confidence level (generally taken as 0.05) indicates significance of the considered term.

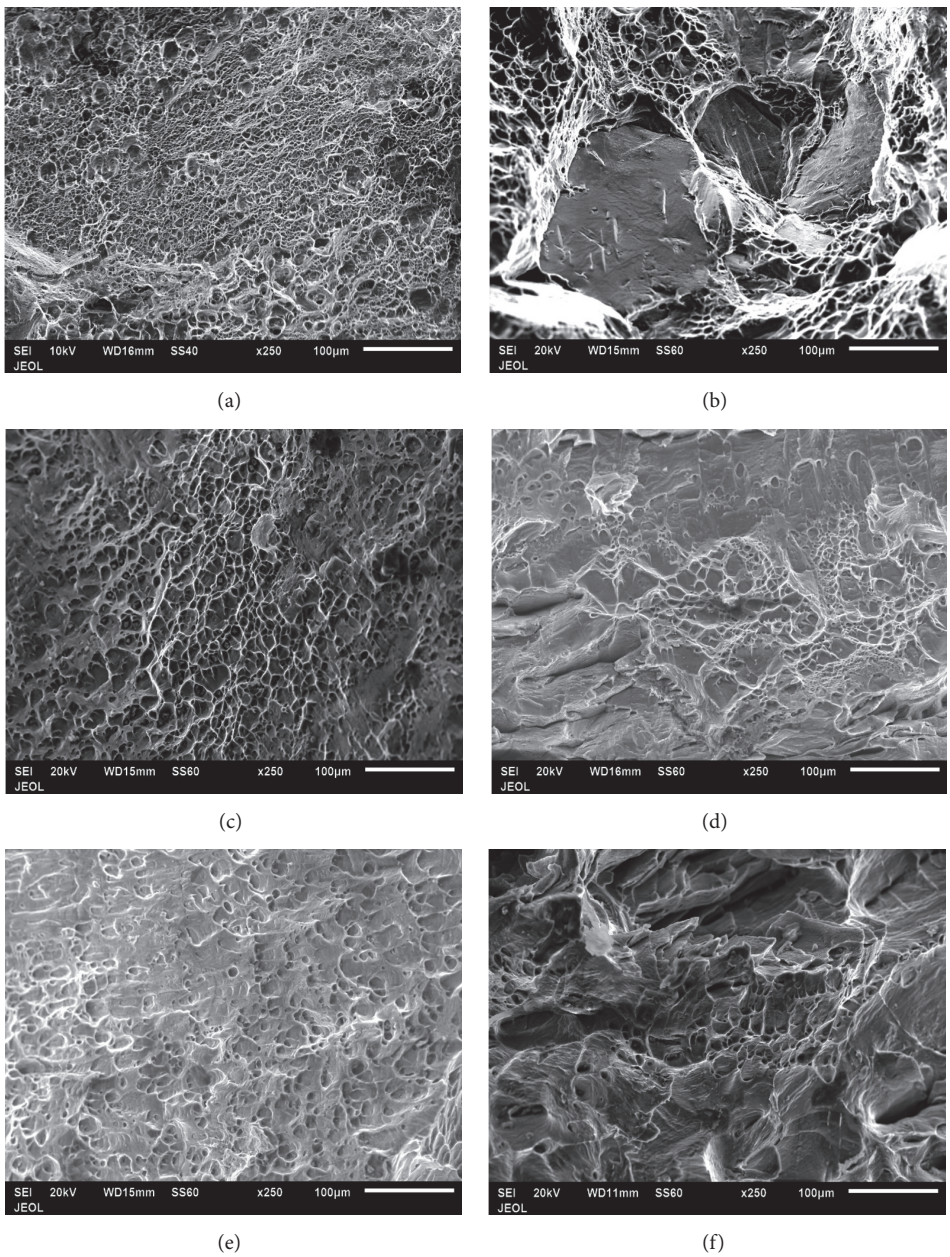

Figure 7: SEM images of the fractured surfaces of Alloy 2 produced by tensile testing: (a) underaged condition tested at room temperature, (b) peak-aged condition tested at room temperature, (c) underaged condition tested at 190°C, (d) peak-aged condition tested at 190°C, (e) underaged condition tested at 250°C, and (f) peak-aged condition tested at 250°C.

The ANOVA results for yield strength are given in Table 8. Model terms with P value > 0.05 are not significant and hence were removed from the model unless they are a part of a higher order interaction or their removal has a significant negative effect on the coefficient of determination (R-squared). The model has an F-value of 23.7 with a P value of about 0.000 implying that the model is significant relative to noise. Significant terms are B (temperature), C (copper content), and the interaction BC. Recall that the effect of C includes the interaction DE (Mg and Ag) as given by the alias structure. Assuming that the third- and fourth-level interactions are negligible, the effects of factor B and interaction BC are calculated with no interference from other terms. The results suggest that aging time and magnesium content do not affect the alloy yield strength. The values of the adjusted sum of squares (Adj. SS) show that the variability in the measured yield strength comes mainly from the copper content and testing temperature.

The model analysis summary is illustrated in Table 9. The adjusted R-squared equal to 0.86 implies that the model represents 86% of the variation in the data. The predicted R-squared was calculated as 0.78, within an acceptable difference from the adjusted R-squared (<0.2), proving that the model is not overfit and has a good predictability.

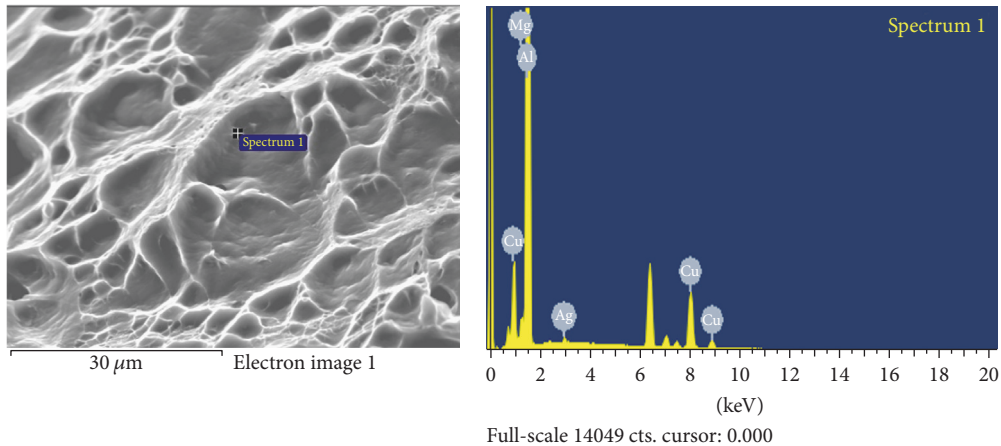

Figure 8: EDS spectrum at the particle taken from fractured surfaces of Alloy 2 peak-aged condition produced by tensile testing at room temperature (Ag: 0.74 wt.%, Mg: 0.76 wt.%, Cu: 20.35 wt.%, and Al: 78.15 wt.%).

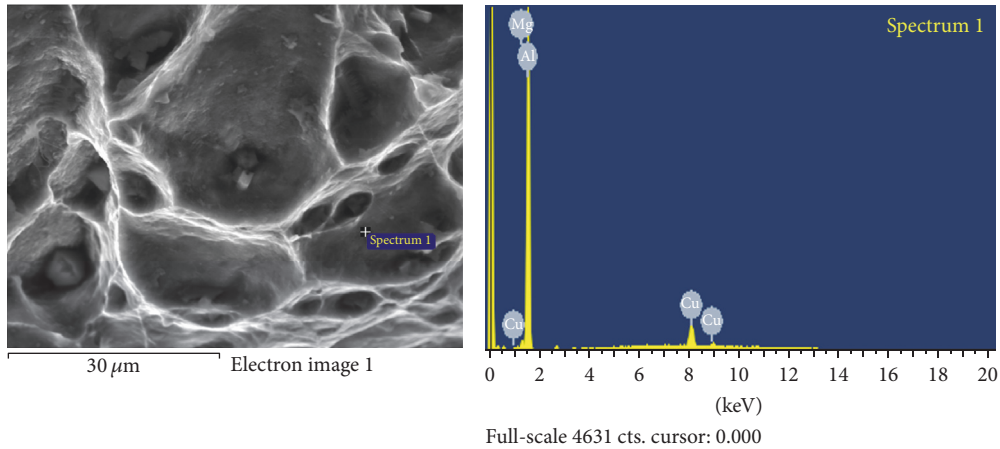

Figure 9: EDS spectrum at the particle taken from fractured surfaces of Alloy 2 peak-aged condition produced by tensile testing at 250°C (Mg: 1.95 wt.%, Cu: 28.96 wt.%, and Al: 69.09 wt.%).

Table 7: The DOE and experimental results for the high-temperature study.

Time	Temp.	Cu	Mg	Ag	Yield strength (MPa)	Ultimate tensile strength (MPa)
A	*B*	*C*	*D*	*E*	*Y*	*U*
−1	−1	−1	−1	1	190	219.7
1	−1	−1	−1	1	250	270.5
−1	1	−1	−1	1	190	201.0
1	1	−1	−1	1	185	194.5
−1	−1	1	−1	−1	315	353.8
1	−1	1	−1	−1	350	372.0
−1	1	1	−1	−1	250	259.5
1	1	1	−1	−1	247	247.1
−1	−1	−1	1	−1	250	310.0
1	−1	−1	1	−1	210	236.6
−1	1	−1	1	−1	200	213.8
1	1	−1	1	−1	190	195.0
−1	−1	1	1	1	295	320.0
1	−1	1	1	1	320	341.0
−1	1	1	1	1	200	220.0
1	1	1	1	1	210	245.0

Table 8: Analysis of variance (ANOVA) results of yield strength for the high-temperature study.

Source	DF	Adj. SS	Adj. MS	F-value	P value
Model	4	38548	9637.1	23.73	0
Linear	3	35008	11669.4	28.74	0
B	1	16129	16129	39.72	0
C	1	17030	17030.2	41.94	0
E	1	1849	1849	4.55	0.056
2-way interactions	1	3540	3540.2	8.72	0.013
$B * C$	1	3540	3540.2	8.72	0.013
Error	11	4467	406		
Total	15	43015			

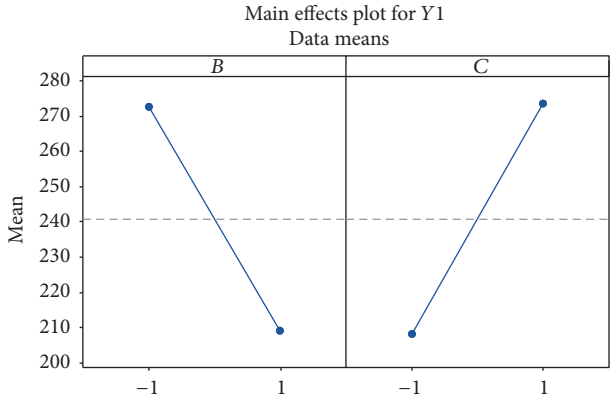

Figure 10: Main effect of significant factors on yield strength for the high-temperature study.

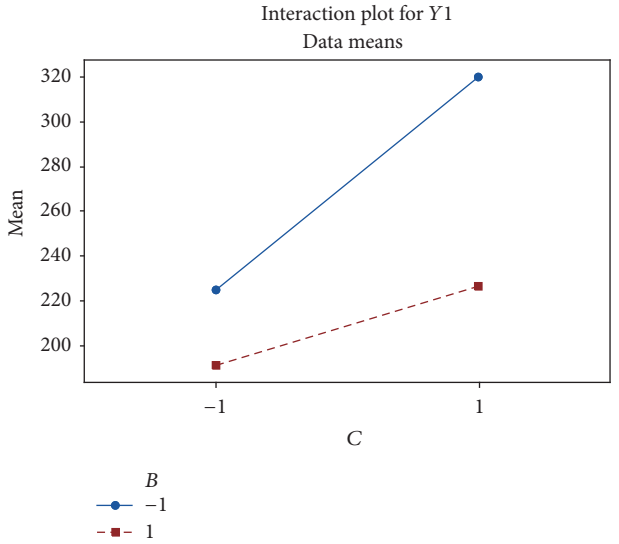

Figure 11: Interaction plot for yield strength for the high-temperature study.

Figures 10 and 11 show the main effect plot and interaction plot for yield strength, respectively. Figure 10 illustrates that increasing the temperature reduces the yield strength, while increasing the copper content increases the yield strength.

Table 9: Model summary of yield strength for the high-temperature study.

S	R-sq.	R-sq. (adj.)	R-sq. (pred.)
20.15	89.62%	85.84%	78.03%

In Figure 11, the interaction is visible as the two lines are not parallel. It is clear that the effect of copper content on increasing the yield strength is reduced as the temperature increases.

Equation (2) gives the regression model for yield strength:

$$Y = -61 + 0.925B + 141.7C - 71.7E - 0.496B * C. \quad (2)$$

The ANOVA results for ultimate tensile strength are given in Table 10. The model has an F-value of 21.7 with a P value of about 0.000 implying that the model is significant relative to noise. Significant terms are B (temperature), C (copper content), E (silver content), and the interactions AE and BC. Recall that the effect of C includes the interaction DE (Mg and Ag) and the effect of E includes the interaction CD as given by the alias structure. Assuming that the third- and fourth-level interactions are negligible, the effects of factor B and interactions BC and AE are calculated with no interference from other terms. The results suggest that aging time and magnesium content do not affect the tensile strength. However, the aging time has an interactive effect with the silver content. The values of the adjusted sum of squares (Adj. SS) show that the variability in the measured ultimate tensile strength comes mainly from the testing temperature followed by the copper content. Previous work [7] reported that the tensile strength did not increase directly with increasing Mg content in Al-Cu-Mg-Ag alloy, which agrees with the current results. On the other hand, though the aging time plays a major role in varying the hardness values, it did not impart a major effect on the tensile properties (yield and ultimate) especially for the testing temperature of 250°C. However, at the 190°C testing temperature, the variation in yield and ultimate strength is present but not with a systematic trend, which could have led to the present statistical prediction of the model. It is worth noting that aging was conducted at 190°C, for all samples; thus, for the testing temperature of 190°C, the effect of under- and peak-aged precipitate conditions was obvious. This effect is

Table 10: Analysis of variance (ANOVA) results of ultimate tensile strength for the high-temperature study.

Source	DF	Adj. SS	Adj. MS	F-value	P value
Model	6	48921.4	8153.6	21.65	0
Linear	4	44883.8	11221	29.8	0
A	1	1	1	0	0.961
B	1	26219.7	26219.7	69.64	0
C	1	16725	16725	44.42	0
E	1	1938.2	1938.2	5.15	0.049
2-way interactions	2	4037.6	2018.8	5.36	0.029
$A * E$	1	1951.4	1951.4	5.18	0.049
$B * C$	1	2086.2	2086.2	5.54	0.043
Error	9	3388.7	376.5		
Total	15	52310.2			

Table 11: Model summary of ultimate tensile strength for the high-temperature study.

S	R-sq.	R-sq. (adj.)	R-sq. (pred.)
19.4043	93.52%	89.20%	79.53%

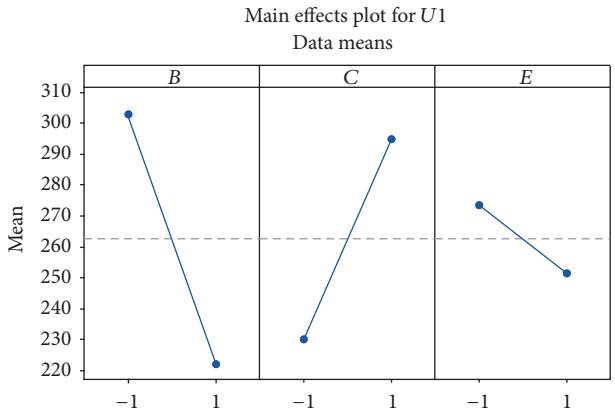

Figure 12: Main effect of significant factors on ultimate tensile strength for the high-temperature study.

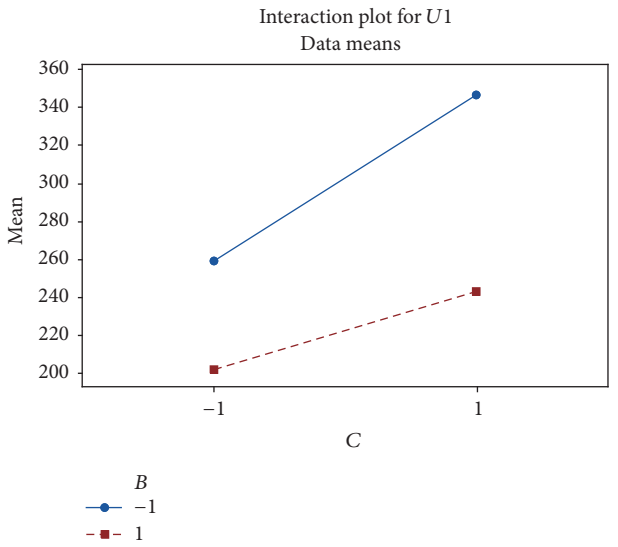

Figure 13: Interaction plot of copper content and temperature BC for ultimate tensile strength for the high-temperature study.

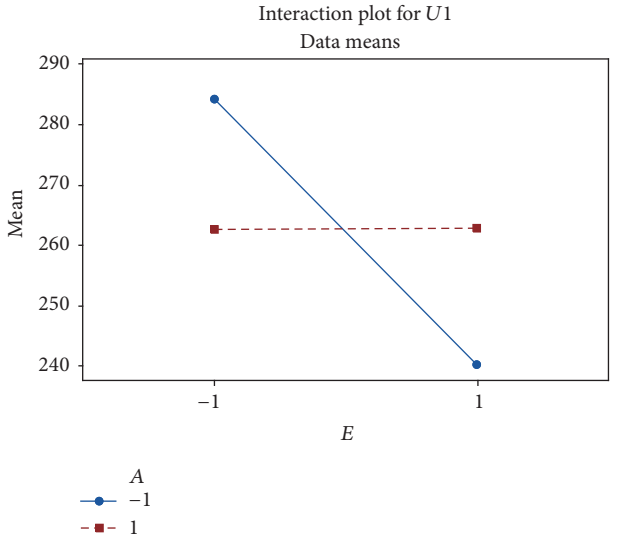

Figure 14: Interaction plot of silver content and time AE for ultimate tensile strength for the high-temperature study.

expected to be less pronounced at higher testing temperature due to the precipitates coarsening that limits the strain hardening processes.

The model analysis summary is illustrated in Table 11. The adjusted R-squared equal to 0.89 implies that the model represents 89% of the variation in the data while the predicted R-squared was calculated as 0.79.

Figures 12 to 14 show the main effect plot and interaction plots, respectively, for ultimate tensile strength. Figure 12 illustrates that increasing the temperature reduces the tensile strength. Increasing the copper content increases the tensile strength while increasing the silver content reduces it. In Figure 13, the interaction is visible as the two lines are not parallel. It is clear that the effect of copper content on increasing the tensile strength is reduced with increasing temperature. Figure 14 shows that although factor A (aging time) is not significant by itself, it seems that increasing

Table 12: Model predicted values versus measured values for validating alloy (Al-3Cu-0.5Mg-0.3Ag) for the high-temperature study.

	Yield strength (MPa)			Ultimate tensile strength (MPa)		
	Measured	Predicted	Relative % error	Measured	Predicted	Relative % error
Underaged (190°C)	200	236	15.3%	239	248	3.6%
Peak-aged (190°C)	240	236	−1.7%	245	292	16.1%
Underaged (250°C)	165	202	18.3%	173	190	9%
Peak-aged (250°C)	160	202	20.8%	173	234	26%

the time at high silver content reduces the tensile strength significantly.

Equation (3) gives the regression model for tensile strength:

$$U1 = 128 + 0.173B + 116.1C - 73.4E + 73.6A * E - 0.381B * C. \quad (3)$$

3.3.1. Validation. To validate the model, an extra alloy was prepared and tested under the same testing conditions as the main designed alloys. The validating alloy had Cu (3 wt.%), Mg (0.5 wt.%), and Ag (0.3 wt.%). The alloy was tested under two temperatures (190 and 250°C) and under two conditions of aging (underaged and peak-aged). The measured yield strength and tensile strength of the alloy are given in Table 12 in comparison to model predicted values. Note that the value of factor A (time) is substituted in the equations as −1 for the underaged condition and +1 for the peak-aged condition, while the other factors are substituted by their actual values.

Paired t-test was used to estimate the significance of the difference between the measured and the predicted values. The test proved no significant difference with P value = 0.081 for the yield strength and 0.074 for ultimate tensile strength. However, as the model was built on a fractional factorial design, it might lack some significant interactions that were omitted in the current study. This may be the reason for some large errors (above 20%) shown in Table 12. A more compressive model should be considered as an extension to this study.

4. Conclusions

Four alloys with different compositions of Al-Cu-Mg-Ag were cast. The alloys were homogenized and hot-rolled. Tensile samples were cut from the rolled sheet. These samples were solution-treated and then aged at 190°C for different aging times comprising underaged and peak-aged conditions. Tensile testing was conducted at room and high temperatures. Changing weight percentages of alloying elements had significant effects on the mechanical properties. The sensitivity of mechanical properties for temperatures was measured through calculating the negative slopes of the yield and ultimate tensile strength variation with temperature.

A mathematical model for the variation of yield strength and ultimate tensile strength was built to relate them with alloying elements content, aging time, and tensile testing temperatures. Both models represent more than 80% of the variation in the data, which represents the reliability of the models. Copper content was most significant for increasing the yield strength and ultimate tensile strength. As expected, increasing temperature reduces the values of YS and UTS.

The promising mechanical properties and the lower sensitivity to high temperatures of Al-Cu-Mg-Ag make them a potential replacement for A2618 and other aluminum alloys used in high-temperature applications such as supersonic aviation and automobile industry.

Conflicts of Interest

The authors declare that they have no conflicts of interest.

Acknowledgments

The authors are thankful to the financial and logistic support of King Abdullah Institute for Nanotechnology and the Deanship of Scientific Research, King Saud University, Riyadh, Saudi Arabia.

References

[1] M. Gazizov and R. Kaibyshev, "Low-cyclic fatigue behaviour of an Al–Cu–Mg–Ag alloy under T6 and T840 conditions," *Materials Science and Technology (United Kingdom)*, pp. 1–11, 2016.

[2] P. Lequeu, "Advances in aerospace aluminum," *Advanced Materials & Processes*, pp. 47–49, 2008.

[3] M. Macar, *Investigation of Dynamics of Behavior of Aluminum Alloy Armor Materials [Ph.D. thesis]*, Middle East technical University, 2014.

[4] J. C. Williams and E. A. Starke Jr., "Progress in structural materials for aerospace systems," *Acta Materialia*, vol. 51, no. 19, pp. 5775–5799, 2003.

[5] J. S. Robinson, R. L. Cudd, and J. T. Evans, "Creep resistant aluminium alloys and their applications," *Materials Science and Technology*, vol. 19, no. 2, pp. 143–155, 2003.

[6] C. L. Lach and M. S. Domack, "Characterization of Al-Cu-Mg-Ag Alloy RX226-T8 Plate," NASA/TM-2003-212639, 2003.

[7] S. Bai, P. Ying, Z. Liu, J. Wang, and J. Li, "Quantitative transmission electron microscopy and atom probe tomography study of Ag-dependent precipitation of Ω phase in Al-Cu-Mg alloys," *Materials Science and Engineering: A*, vol. 687, pp. 8–16, 2017.

[8] S. Bai, X. Zhou, Z. Liu, P. Xia, M. Liu, and S. Zeng, "Effects of Ag variations on the microstructures and mechanical properties of Al-Cu-Mg alloys at elevated temperatures," *Materials Science and Engineering A*, vol. 611, pp. 69–76, 2014.

[9] D. Bakavos, P. B. Prangnell, B. Bes, and F. Eberl, "The effect of silver on microstructural evolution in two 2xxx series Al-alloys

with a high Cu:Mg ratio during ageing to a T8 temper," *Materials Science and Engineering A*, vol. 491, no. 1-2, pp. 214–223, 2008.

[10] R. N. Lumley and I. J. Polmear, "The effect of long term creep exposure on the microstructure and properties of an underaged Al-Cu-Mg-Ag alloy," *Scripta Materialia*, vol. 50, no. 9, pp. 1227–1231, 2004.

[11] B. M. Gable, G. J. Shiflet, and J. Starke, "Alloy development for the enhanced stability of Ω precipitates in Al-Cu-Mg-Ag alloys," *Metallurgical and Materials Transactions A: Physical Metallurgy and Materials Science*, vol. 37, no. 4, pp. 1091–1105, 2006.

[12] D. H. Xiao, J. N. Wang, D. Y. Ding, and H. L. Yang, "Effect of rare earth Ce addition on the microstructure and mechanical properties of an Al-Cu-Mg-Ag alloy," *Journal of Alloys and Compounds*, vol. 352, no. 1-2, pp. 84–88, 2003.

[13] S. Bai, Z. Liu, Y. Li, Y. Hou, and X. Chen, "Microstructures and fatigue fracture behavior of an Al-Cu-Mg-Ag alloy with addition of rare earth Er," *Materials Science and Engineering A*, vol. 527, no. 7-8, pp. 1806–1814, 2010.

[14] A. Cho and B. Bes, "Damage tolerance capability of an Al-Cu-Mg-Ag alloy(2139)," *Materials Science Forum*, vol. 519-521, no. 1, pp. 603–608, 2006.

[15] M. Song, K.-H. Chen, and L.-P. Huang, "Effects of Ag addition on mechanical properties and microstructures of Al-8Cu-0.5Mg alloy," *Transactions of Nonferrous Metals Society of China (English Edition)*, vol. 16, no. 4, pp. 766–771, 2006.

[16] Q. K. Xia, Z. Y. Liu, and Y. T. Li, "Microstructure and properties of Al-Cu-Mg-Ag alloy exposed at 200°C with and without stress," *Transactions of Nonferrous Metals Society of China (English Edition)*, vol. 18, no. 4, pp. 789–794, 2008.

[17] X. Y. Liu, Q. L. Pan, X. L. Zhang et al., "Creep behavior and microstructural evolution of deformed Al-Cu-Mg-Ag heat resistant alloy," *Materials Science and Engineering A*, vol. 599, pp. 160–165, 2014.

[18] R. N. Lumley, A. J. Morton, and I. J. Polmear, "Enhanced creep performance in an Al-Cu-Mg-Ag alloy through underageing," *Acta Materialia*, vol. 50, no. 14, pp. 3597–3608, 2002.

[19] A. M. Al-Obaisi, E. A. El-Danaf, A. E. Ragab, and M. S. Soliman, "Precipitation Hardening and Statistical Modeling of the Aging Parameters and Alloy Compositions in Al-Cu-Mg-Ag Alloys," *Journal of Materials Engineering and Performance*, pp. 1–13, 2016.

[20] J. C. Lourenço, M. I. S. T. Faria, A. Robin, L. P. Prisco, and M. C. Puccini, "Influence of process parameters on localized corrosion of AA7075 alloy during the production of aeronautic components," *Materials and Corrosion*, vol. 66, no. 12, pp. 1498–1503, 2015.

[21] T. A. El-Taweel and S. Haridy, "An application of fractional factorial design in wire electrochemical turning process," *International Journal of Advanced Manufacturing Technology*, vol. 75, no. 5-8, pp. 1207–1218, 2014.

[22] E. M. Salleh, H. Zuhailawati, S. Ramakrishnan, and M. A.-H. Gepreel, "A statistical prediction of density and hardness of biodegradable mechanically alloyed Mg-Zn alloy using fractional factorial design," *Journal of Alloys and Compounds*, vol. 644, pp. 476–484, 2015.

[23] I. J. Polmear and M. J. Couper, "Design and development of an experimental wrought aluminum alloy for use at elevated temperatures," *Metallurgical Transactions A*, vol. 19, no. 4, pp. 1027–1035, 1988.

[24] K. M. Knowles and W. M. Stobbs, "The structure of 111 age-hardening precipitates in Al–Cu–Mg–Ag alloys," *Acta Crystallographica Section B*, vol. 44, no. 3, pp. 207–227, 1988.

[25] B. C. Muddle and I. J. Polmear, "The precipitate Ω phase in Al-Cu-Mg-Ag alloys," *Acta Metallurgica*, vol. 37, no. 3, pp. 777–789, 1989.

[26] A. Garg, Y. C. Chang, and J. M. Howe, "Precipitation of the Ω phase in an Al-4.0Cu-0.5Mg alloy," *Scripta Metallurgica et Materiala*, vol. 24, no. 4, pp. 677–680, 1990.

[27] M. Grujicic, G. Arakere, C.-F. Yen, and B. A. Cheeseman, "Computational investigation of hardness evolution during friction-stir welding of AA5083 and AA2139 aluminum alloys," *Journal of Materials Engineering and Performance*, vol. 20, no. 7, pp. 1097–1108, 2011.